Crack Propagation in Layered Ceramic Composites of Alumina and Mullite

Henryk Tomaszewski, Marek Boniecki and Helena Weglarz

Institute of Electronic Materials Technology,
Wolczynska 133, 01-919 Warsaw, Poland

ABSTRACT

Laminar composites, containing layers of Al_2O_3 and either mullite or a mixture of mullite and Al_2O_3, were fabricated using a sequential centrifuging technique of water solutions containing suspended particles. Controlled crack growth experiments with notched beams of composites showed the significant effect of barrier layer thickness and composition on the crack propagation path during fracture. Distinct crack deflection in mullite layers was observed. Also, an increase of the crack deflection angle with the mullite layer thickness was found. In the case of barrier layers made of a mixture, crack deflection was not found independent of layer thickness. The observed changes were correlated with the distribution of residual stresses in layers created during cooling of sintered composites from their fabrication temperature. These residual stresses are a result of thermal expansion and subsequent sintering shrinkage mismatch of alumina and mullite.

Keywords: layered composite, crack deflection, fracture toughness

1. INTRODUCTION

Ceramic materials are naturally brittle, so much effort has been directed to improve their toughness by various methods. Since the discovery of transformation toughening in ZrO_2 in 1975 /1/, a variety of toughened ZrO_2-based materials have been developed. Models /2-4/ predict that the increase in toughness is linked with the size and shape of the transformation zone. A new way of optimising the transformation zone was developed by Marshall *et al.* /5,6/ in multilayered ceramic composites. A significant toughness increase of a Ce-TZP matrix with Al_2O_3 or Al_2O_3/ZrO_2 barrier layers was attributed to spreading of the transformation zone. In contrast with Marshall's results, Tomaszewski *et al.* /7,8/ showed that the main mechanism responsible for the toughness increase in ZrO_2-based laminated composites is crack deflection in the barrier layers caused by the presence of residual stress. The extent of the toughness increase was dependent on both layer thickness and on composition. A correlation between crack deflection and distribution of compressive residual stresses in barrier layers of composites was also found.

In order to confirm these observations, alumina/mullite layered composites were prepared in the present work. In the mullite layer with lower thermal expansion coefficient, α, ($\alpha_{mullite}=5x10^{-6}\ ^oC^{-1}$) a biaxial compressive residual stress is expected (Fig. 1) and similarly, a biaxial tensile residual stress in the alumina layer with higher α ($\alpha_{Al2O3}=9x10^{-6}\ ^oC^{-1}$). The tensile residual stress in the alumina layer is expected to promote crack opening in the notched beam during bending. Conversely, the compressive residual stress in the mullite layer will prevent opening of the crack.

2. EXPERIMENTAL PROCEDURE

Composites of Al_2O_3/mullite with 25-75μm thick layers were fabricated by sequential centrifuging (Model Z382, Hermle) of powder suspensions (Table I). Aqueous slurries containing 5 to 10wt% of powder were prepared by ultrasonicating the powders in deionized water at pH 4. Cast samples were dried, additionally

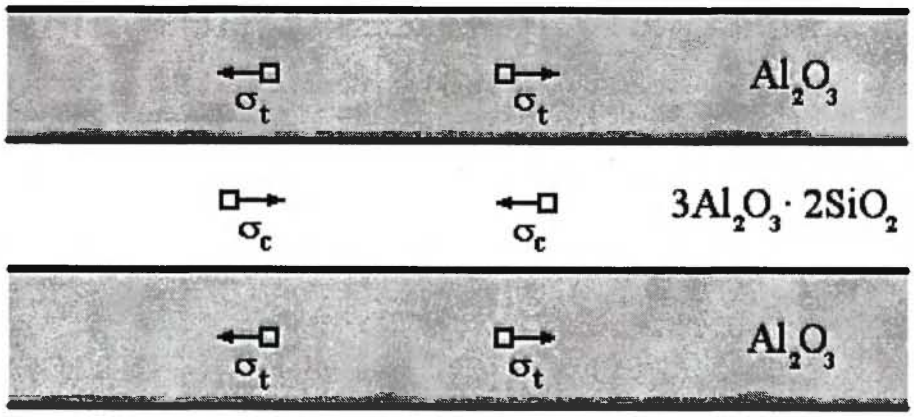

Fig. 1: Expected residual stress distribution in layered alumina/mullite composite: σ_t – tensile stresses, σ_c – compressive stresses

Table I
Ceramic powders used for preparing layered composites

Powder type	Producer	Grain size, μm	Sintering shrinkage, %	Application
Alumina	CEMAT, Poland	0.5	22.3	Matrix layer
Mullite SASM	Baikowski Chimie, France	0.7	18.4	Barrier layer

isostatically pressed at 120MPa and then sintered at 1700°C. To minimise the shrinkage mismatch of Al_2O_3 and mullite, in some layered composites a mixed composition of 50vol% alumina and mullite was used instead of pure mullite. After sintering the samples were cut and ground to the dimensions of 45x5x5mm^3 or 45x6x1.5mm^3 and one surface perpendicular to the layers was polished. The sharp notch perpendicular to layers in the centre of the beams was prepared with two diamond saws: 0.200 and 0.025mm thick.

The bending strength of the composites was determined on square bars with dimensions 45x5x5mm^3 in three-point bending tests using a universal testing machine (Model 1446, Zwick) with 1mm/min loading speed and 40mm bearing distance.

For measurement of Young's modulus the beams were trimmed to a height of 1mm and then the compliance of the samples was recorded during loading tests with 0.1mm/min loading speed and 40mm bearing distance. The values of Young's modulus were determined using the relationship given by Fett and Munz /9/, which is stated in equation (3) below.

The critical stress intensity factor, K_{Ic}, was measured following Evans /10/ on notched beams (45x1.5x6mm^3, notch ~1mm) perpendicularly to the layers in a three-point bending test. The bearing spacing was 40mm and rate of loading 1mm/min.

Controlled crack growth tests were performed in three-point bending with 1μm/min loading speed and 40mm bearing distance using the same testing machine. The crack was initiated and slowly grown by repeated loading and unloading. The procedure results in an increase of crack length per step of less than 100μm. The crack length, c, was measured *in situ* using a special device consisting of a horizontal light microscope coupled with a CCD camera which were fitted to the testing machine by a system of elevator stages driven by stepping motors. This enabled the precise movement of the microscope objective in x-y-z directions for adjustment, focussing and tracking on the specimen side

and bottom surface where the crack propagated. A measuring and registration system (framegrabber) was coupled to the testing machine, and a computer controlled both systems. The magnification was about 250x.

The stress intensity factor, K_I, was calculated from the crack length, c, and the force, P. The data of $K_I = f(c)$ obtained in the range of crack length studied were fitted by a linear function $y=ax+b$ and the slope, a, was used as a parameter describing R-curve behaviour. All experiments were done at room temperature in ambient air environment.

In several samples the crack growth tests were done without unloading. The time dependent displacement, d, of the sample was measured and recorded together the force, P. According to Fett and Munz /9/, the total compliance, C, (which is given by equation (1))

$$C = \frac{d}{P} \tag{1}$$

consists of the compliance of the loading system, C_u, the compliance of the uncracked specimen, C_0, and the portion ΔC caused by the crack.

$$C = C_u + C_0 + \Delta C \tag{2}$$

$$\text{with} \quad C_0 = \frac{L^2}{w^2 BE}\left[\frac{L}{4w} + (1+\nu)\frac{w}{2L}\right] \tag{3}$$

where E is Young's modulus, ν is Poisson's ratio, w is the specimen thickness, B is the specimen width and L is the bearing distance. The compliance due to the crack was calculated using /9/ as

$$\Delta C = 4.5\frac{L^2}{w^2 EB}\left(\frac{a}{1-a}\right)^2 \sum_{i=0}^{5}\sum_{j=0}^{3} B_{ij} a^i \left(\frac{w}{L}\right)^j \tag{4}$$

with $a = \frac{c}{w}$, where c is the length of the crack and B_{ij} are the coefficients given by Fett and Munz /9/.

The stress intensity factor K_I values have been determined from the relation (5)

$$K_I = 1.5\frac{PL}{w^2 B} Y c^{\frac{1}{2}} \tag{5}$$

using the geometric function Y, stated below in equation (6), with the coefficients A_{ij} given by Fett and Munz /9/.

$$Y = \frac{\sqrt{\Pi}}{(1-a)^{3/2}}\left[0.3738a + (1-a)\sum_{i,j=0}^{4} A_{ij} a^i \left(\frac{w}{L}\right)^j\right] \tag{6}$$

By this procedure the maximal stress intensity factor, K_{Imax}, and the resistance to crack initiation, K_{Ii}, were calculated. The crack growth rate $v=dc/dt$ was calculated from the time dependent crack length, c. Assuming a power-law relation between v and K_I (equation 7), the parameters A (or $logA$) and n were obtained.

$$v = \frac{dc}{dt} = AK_I^n \tag{7}$$

Given that the area under the recorded load-deflection curve of the specimen is the sum of the work used for the creation of two new surfaces and the elastic strain energy of the system and sample studied, the work-of-fracture, γ_F, was determined:

$$\gamma_F = U/2A \tag{8}$$

where U is the total deformation work of a specimen up to fracture and A is the area of fractured cross-section of the specimen.

Microstructure observations were performed on polished surfaces by SEM using an OPTON DSM950 microscope.

3. RESULTS

The controlled crack growth experiments indicated significant crack deflection in barrier layers of composites dependent on barrier thickness and composition, similarly to the results obtained for zirconia/alumina composites /7,8/. Cracks were only deflected in the mullite layers (Fig. 2) subjected to compressive residual stress. In alumina layers the crack deflects back to its original direction perpendicular to the layers. The degree of crack deflection depends on the mullite layer thickness. As can be seen from Table II, the crack deflection angle increases with layer

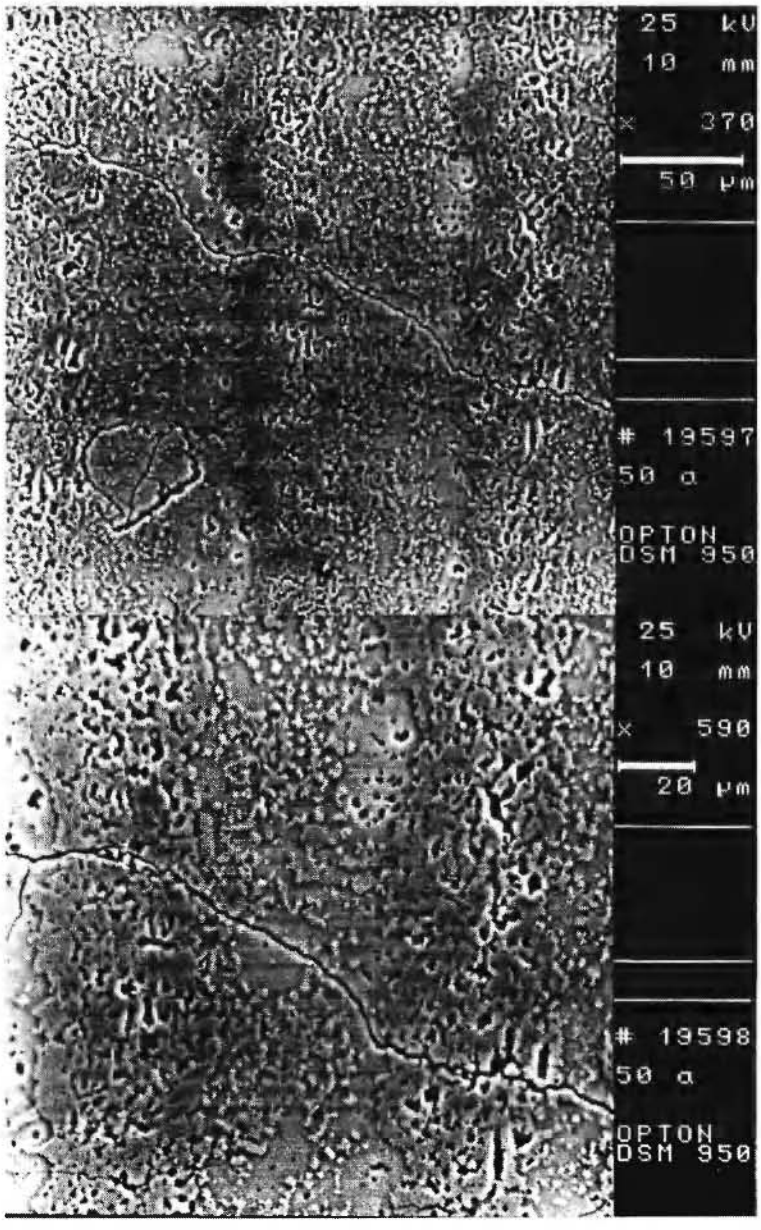

Fig. 2: Crack path in Al_2O_3/mullite composite with 50µm thick mullite barrier layers: the crack is deflected in mullite layers, in alumina layers (layer with pores) it propagates perpendicularly to the layers.

Table II

Crack deflection angle measured in the mullite layers of an alumina/mullite composite as a function of layer thickness

Thickness of mullite layer,µm	25	50	75
Crack deflection angle, °	0	48±5	90

thickness. For example, in a 75μm thick mullite layer the crack deflects over 90°. In layers with a thickness of 25μm and lower, deflection does not take place.

The character of the crack path changed strongly in composites with barrier layers made of a mullite and alumina mixture instead of pure mullite. Figs. 3 and 4 show that the crack propagates through the barrier layers without deflection, for all the layer thicknesses studied.

Thickness dependent crack deflection in mullite layers results in an increase in the slope parameter, *a*, describing the R-curve behaviour of the composites. As can be seen from Table III, the value of *a* equals 1.02 and 1.829 for composites with 50μm and 75μm thick mullite layers, respectively. For composites with a mixed barrier layer the corresponding values are 0.402 and 0.641. Deflection can be regarded as a more effective mechanism in increasing the fracture

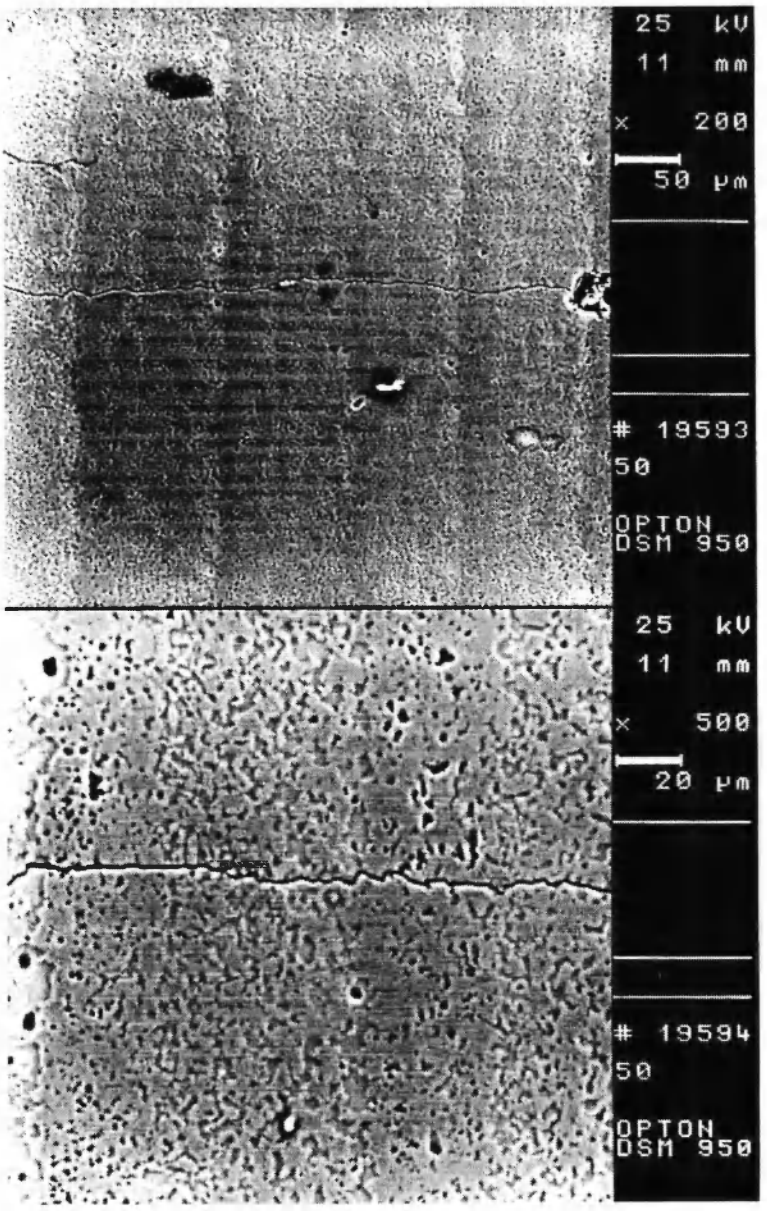

Fig. 3: Crack path in Al_2O_3/mullite composite with 50μm thick barrier layers made of a mullite and alumina mixture

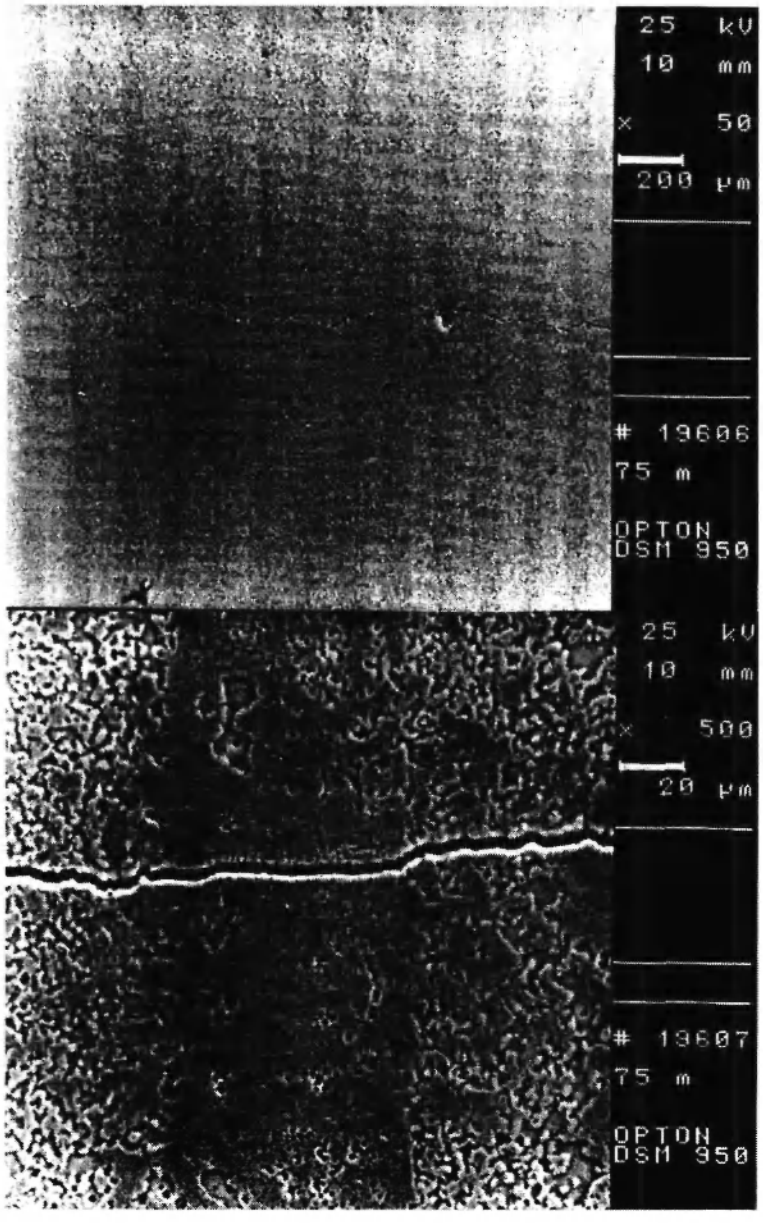

Fig.4. Crack path in Al_2O_3/mullite composite with 75µm thick barrier layers made of a mullite and alumina mixture

Table III

Linear coefficients *a* and *b* (equation $K_I=ac+b$) for layered composites of alumina and mullite and of alumina and alumina/mullite mixture

Type of barrier layers	Mullite		Mixture of mullite and alumina	
Layer thickness, µm	50	75	50	75
a	1.0±0.2	1.8±0.4	0.4±0.1	0.6±0.1
b	1.8±0.4	1.6±0.6	3.6±0.4	3.2±0.5

toughness as the crack growth (see Fig. 5) than the bridging mechanism present in pure alumina. Indeed the parameter a for a pure alumina matrix is 0.606 (see Fig. 6 and Table IV), which means that the toughness increases strongly namely from 3.6 to about 5.5 $MPam^{1/2}$ as the crack length increases up to 4.2mm.

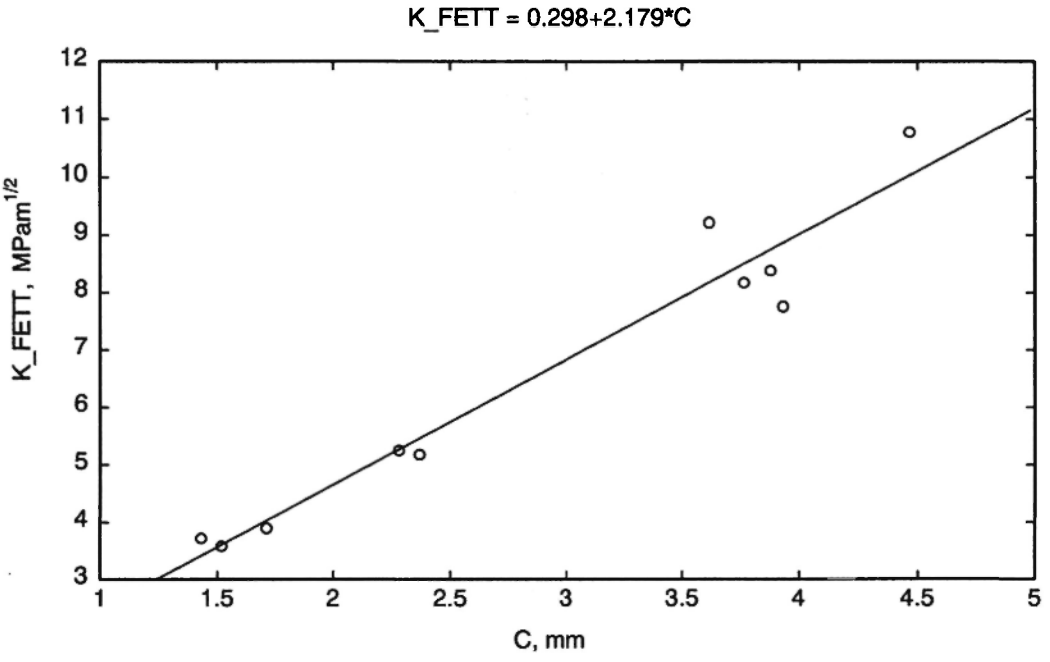

Fig. 5: Dependence of K_I on the crack length for a layered composite of alumina and mullite with 75μm. thick mullite layers.

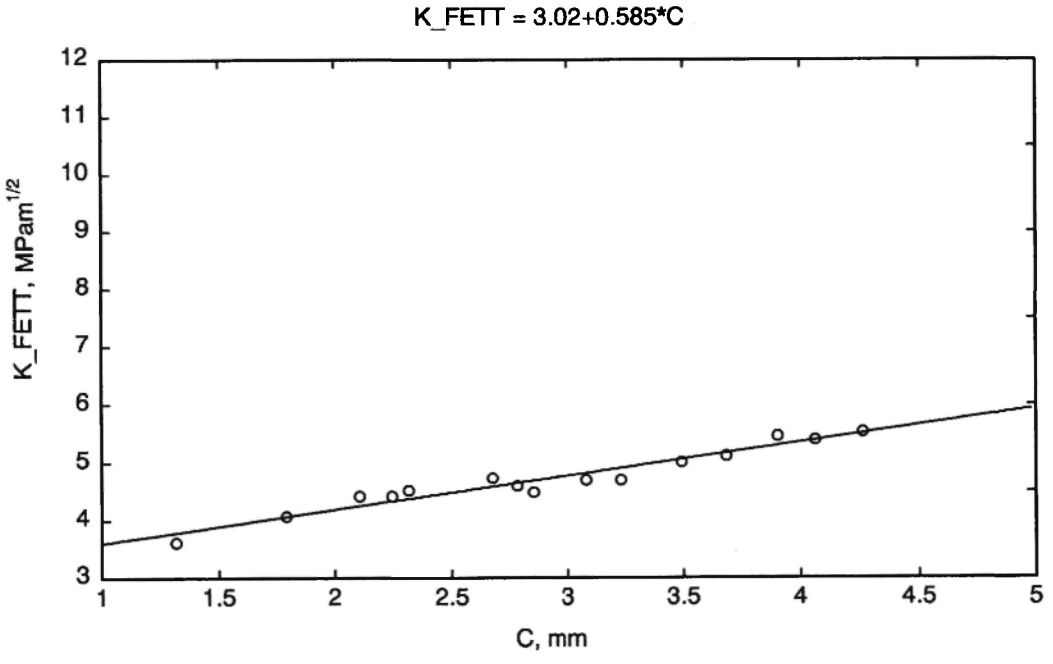

Fig. 6: Dependence of K_I on the crack length for an alumina matrix as used in the preparation of the layered composite

Table IV
Linear coefficients a and b (equation $y=ax+b$) for alumina, mullite and a mixture of mullite and alumina

Type of ceramics	a	b
Alumina	0.61+0.02	3.05±0.03
Mullite	-0.06±0.01	1.78±0.01
Mixture of mullite and alumina	0.12±0.05	2.82±0.09

However the increase in matrix toughness becomes less pronounced when mullite is added. For a mixed composition of 50vol% alumina and mullite, the slope parameter decreases to 0.118. This decrease in parameter a suggests that mullite changes the residual stress state in the alumina matrix. The large thermal expansion mismatch between mullite and Al_2O_3 is thought to create additional regions of tension, as was found in Al_2O_3-SiC system /11/. This in turn reduces the effectiveness of grain bridging and in consequence, the slope parameter a.

Crack deflection in mullite layers results also in an increase in toughness of the composites. Table V shows that the critical stress intensity factor, K_{Ic}, work-of-fracture, γ_F, and bending strength, σ_b, increase with mullite barrier layer thickness and reach a maximum for the thickest layers. In the case of the thinnest layers, where crack deflection is not observed, the properties do not differ from the values obtained for composites with mixed barrier layers. Similar changes are observed in the maximal stress intensity factor K_{Imax}, in the resistance to crack initiation K_{Ii} and in the crack growth rate parameter n. The decreasing values of parameter n show that crack will propagate at a lower rate in composites with thicker mullite layers than in composites with the thinner layers. For comparison, properties of alumina, mullite and a homogenised mixture of mullite and alumina are presented in Table VI. The critical stress intensity factor of mullite, the resistance to crack initiation and the bending strength are substantially lower than for alumina. On the other hand, the fracture toughness of a homogenised mixture of mullite and alumina is not distinctly different from that of alumina ceramics. This can be a result of residual stresses present in this composite, with alumina grains in tension and mullite grains in compression. Local compressive stress fields created by mullite grains may be responsible for the moderate decrease of bending strength compared to pure alumina.

However the large difference in fracture toughness

Table V
Mechanical properties of layered composites of alumina and mullite as a function of barrier layer thickness and composition

Type of barrier layer	Mullite			Mixture of mullite and alumina	
Layer thickness,μm	25	50	75	50	75
γ_F, J/m^2	26.7±2.4	57.5±1.1	76.2±1.3	39.4±5.9	40.4±4.6
K_{Ic}, MPam$^{1/2}$	4.14±0.52	4.55±0.22	5.85±0.19	3.87±0.31	4.27+0.53
σ_b, MPa	228.9±49.0	287.1±19.0	361.5±7.8	221.2+21.4	201.7+15.7
K_{Imax}, MPam$^{1/2}$	4.61±0.30	4.94±0.17	5.44±0.10	5.09±0.33	5.09+0.06
K_{Ii}, MPam$^{1/2}$	2.72±0.18	3.48±0.43	3.72±0.42	2.67+0.19	2.89±0.30
n	18.8±3.2	16.2±5.0	7.1±1.3	27.7+2.2	31.8±2.5
logA	-15.8±3.2	-14.9±3.9	-8.8±0.1	-20.6+2.4	-25.9±2.4

Table VI
Mechanical properties of alumina, mullite and a mixture of mullite and alumina

Type of ceramics	Alumina	Mullite	Mixture of mullite and alumina
K_{Ic}, MPam$^{1/2}$	3.93+0.06	2.41±0.08	3.62±0.04
σ_b, MPa	328.5±25.5	153.5±12.5	277.5+26.4
K_{Imax}, MPam$^{1/2}$	5.06±0.04	2.27+0.07	3.64+0.25
K_{Ii}, MPam$^{1/2}$	2.96±0.09	1.75±0.17	2.76±0.04

between layered and homogenised composites with the same volume fraction of mullite and alumina (see Tables V and VI) seems to be a confirmation of the effect of crack deflection and of the role of residual stress distribution in polycrystalline ceramics.

4. DISCUSSION

Observations made by Ho *et al.* /12/ and Oechsner *et al.* /13/ show that the stress state near the surface of a laminar composite specimen as presented in Fig. 1 is more complex. These authors found edge cracks on the surface of thin layers that were under nominal, residual compressive stress caused by the biaxial constraint of an adjacent, thicker layer with a larger α. These edge cracks appear near the centre of the layer, propagate into the layer and run parallel to the centreline. They showed that although biaxial residual compressive stresses exist in the layer far from the free surface, the residual stress distribution near the free surface is triaxial. Specifically, the component of the triaxial stress perpendicular to the centreline of the layer is a highly localised tensile stress, which diminishes in magnitude from the surface to the interior. Ho *et al.* /12/ observed that the occurrence of edge cracks depended on the thickness of the internal layer and on the magnitude of the residual compressive stress in it. They found also that for a given residual stress, crack extension without any applied stress takes place only when the thickness of the external layer exceeds a critical value.

In our study the thickness of matrix and barrier layer is equal (25 to 75μm) and edge cracks parallel to the layer were not found. In our opinion, crack deflection in mullite barrier layers results from the interaction of three types of stress. The first is a residual compressive stress acting in the plane parallel to the layers and is caused by the thermal expansion mismatch. The second is a perpendicular tensile stress found by Ho *et al.* /12/ and Oechsner *et al.* /13/. Both of these stress types are present in a laminate after cooling from fabrication temperature. The third is the external tensile stress applied in bending of the notched beam. An additional factor responsible for crack deflection can then be the compressive stress distribution in barrier layers. As found in layered composites of ZrO_2 and Al_2O_3 /7,8/, the maximum compressive stress occurs at the interface between layers and minimum in the centre of the mullite barrier layer. The magnitude of the minimum stress depends on layer thickness. According to Ho *et al.* /12/ and Oechsner *et al.* /13/, the maximum of normal tensile stress exists in the centre of the barrier layer and also depends on layer thickness. This means that in the centre of the barrier layers above a critical thickness the perpendicular tensile stress dominates. As a result, the crack deflects in the centre of the thick layer and propagates along the layer. The compressive stress increases from the minimum in the centre to the maximal value at the interface, then the crack deflects back to the original direction. For the thinnest barrier layer the compressive stress across the layer is almost constant (the stress difference is at a minimum) but when perpendicular tensile stress in the centre reaches a minimum value the crack propagates through the layer without deflection. For intermediate thickness, deflection of the crack at an angle of less than 90° is a result of combined stresses.

5. SUMMARY

The aim of this work was to investigate layered ceramic composites made of alumina matrix layers and mullite or mullite/alumina barrier layers. A distinct enhancement of toughness was found only for the composite with mullite barrier layers. Controlled crack growth tests showed that the only mechanism responsible for the toughness increase is crack deflection. The degree of deflection was proportional to the mullite layer thickness. In the case of layer thickness below 25μm the crack was not deflected. Crack deflection was not observed in the layers made of a mixture independently of layer thickness. An explanation for this phenomenon was given by analysis of the stresses present in the composite. These results agree with similar observations found in layered composites of alumina and zirconia, namely that crack deflection in the barrier layers is a result of residual stresses generated by thermal expansion mismatch.

6. REFERENCES

1. R.C. Garvie, R.H.J. Hannink and R.T. Pascoe, "Ceramic steel?", *Nature (London)*, **258**, 703-704 (1975).
2. A.G. Evans and R.M. Cannon, "Toughening of brittle solids by martensitic transformations" *Acta Metall.*, **34** (5), 761-800 (1986).
3. R.M. McMeeking and A.G. Evans, "Mechanics of transformation-toughening in brittle materials", *J. Amer. Ceram. Soc.*, **65** (5) 242-246 (1982).
4. J.C. Lambropoulos J.C., "Effect of nucleation on transformation toughening", *J. Amer. Ceram. Soc.*, **69**, (3), 218-222 (1986).
5. D.B. Marshall, F.F. Lange and J.J. Ratto, "Enhanced fracture toughness in layered microcomposites of Ce-ZrO_2 and Al_2O_3", J. *Amer. Ceram. Soc.*, **74** (12), 2979-87 (1991).
6. D.B. Marshall, "Design of high-toughness laminar zirconia composites", *Ceram. Bull.*, 71, (6), 969-973 (1992).
7. H. Tomaszewski, J. Strzeszewski. and W. Gebicki, "The role of residual stresses in layered composites of Y-ZrO_2 and Al_2O_3", *J. Europ. Ceram. Soc.*, **19**, 255-262 (1999).
8. H. Tomaszewski, H. Weglarz, M. Boniecki and W.M. Recko, "Effect of barrier layer thickness and composition on fracture toughness of layered zirconia/alumina composites", *J. Mat. Sci.*, **35** (16), 4165-4176 (2000).
9. T.F. Fett and D. Munz, "Subcritical crack growth of macrocracks in alumina with R-Curve behaviour", *J. Amer. Ceram. Soc.*, **75**, (4), 958-963 (1992).
10. R.C. Bradt, D.P.H. Hasselman and F.F. Lange, "Fracture mechanics determination", in: *Fracture Mechanics of Ceramics*, vol.1, Plenum Press, 1974; 17-48.
11. H. Tomaszewski, M. Boniecki and H. Weglarz, "Toughess-curve behaviour of alumina-SiC and ZTA-SiC composites", *J. Europ. Ceram. Soc.*, **20**, 1215-1224 (2000).
12. S. Ho, C. Hillman, F.F. Lange and Z. Suo, "Surface cracking in layers under biaxial residual compressive stress", *J. Amer. Ceram. Soc.*, **78**, (9), 2353-2359 (1995).
13. M. Oechsner, C. Hillman and F.F. Lange, "Crack bifurcation in laminar ceramic composites", *J. Amer. Ceram. Soc.*, **79**, (7), 1834-1838 (1996).